Determination of lattice parameter and of N lattice location in $In_xGa_{1-x}N_yAs_{1-y}$/GaAs and GaN_yAs_{1-y}/GaAs epilayers

G. Bisognin, D. De Salvador, C. Mattevi, M. Berti,[a] and A. V. Drigo
INFM and Department of Physics, University of Padova, Via Marzolo 8, I-35131 Padova, Italy

G. Ciatto
INFM c/o ESRF-Gilda CRG, 6 rue J. Horowitz, BP 220, 38043 Grenoble, France

L. Grenouillet, P. Duvaut, and P. Gilet
CEA-DRT-LETI/DOPT-CEA/GRE, 17, avenue des Martyrs, 38054 Grenoble Cedex 9, France

H. Mariette
Group "Nanophysique et Semiconducteurs" Laboratoire de Spectrometrie Physique, Universite J. Fourier–Grenoble-I, BP87, France

(Received 23 June 2003; accepted 1 October 2003)

We have used an experimental strategy that, combining nuclear reaction analysis and Rutherford backscattering spectrometry both in random and channeling geometry, allowed an accurate quantification of the total amount of N in $In_xGa_{1-x}N_yAs_{1-y}$/GaAs and GaN_yAs_{1-y}/GaAs epitaxial systems ($0.038<x<0.044$, $0.015<y<0.045$), and a precise localization of nitrogen atoms into the lattice. All N atoms were found on substitutional positions. This information was then exploited to correlate the relaxed lattice parameter of the epilayers obtained by high-resolution x-ray diffraction to the N concentration, by taking into account the elasticity theory, allowing a verification of the validity of Vegard's rule in the whole range of investigated N concentrations for both alloys. The effect of N incorporation on the lattice parameter has been found to be the same both for ternary and quaternary alloys. © *2004 American Institute of Physics.* [DOI: 10.1063/1.1628378]

I. INTRODUCTION

Group III N-As alloys have recently attracted a lot of interest because very low N concentrations cause a large decrease in the bandgap, making these materials very attractive for applications in optoelectronic devices.[1–7] Moreover, as small N concentrations induce large tensile strain that can be compensated by the addition of In, quaternary InGaNAs alloys can be grown lattice matched to GaAs substrates.

However, it has been shown that the as-grown materials have poor photoluminescence (PL), and that the higher the N concentration the lower the PL efficiency.[8] As after rapid thermal annealing the PL efficiency is greatly increased, the poor PL property of the as-grown material was attributed to N-related nonradiative defects possibly associated with some kinds of N interstitials.[2,9]

Neugebauer and Van de Walle,[10] on the basis of local density approximation, have shown that Vegard's rule is valid when N is substituted for As. On the other hand, increasing deviations from Vegard's rule have been experimentally found for increasing N concentrations,[2,9,11] and attributed to N incorporation in other locations than the group V lattice sites or to [001] split interstitial complexes like N-As or N-N. However, opposite deviations from the Vegard's rule have been found in Refs. 2, 9, and 11.

All these facts indicate that the precise characterization of the structural properties of the alloys is of paramount importance in order to understand and tailor their physical properties. To this purpose, the use of high-resolution x-ray diffraction (HRXRD), secondary ion mass spectroscopy (SIMS), nuclear reaction analysis (NRA), and Rutherford backscattering spectrometry (RBS) both in random and channeling geometry have been already reported.[1,2,11,12] As the total amount of N to be detected is very small (on the order of few atomic monolayers) particular attention must be paid to possible artifacts and contaminations that could lead to misinterpretation of the results. The aim of this article is twofold: first, a careful assessment of the nuclear techniques and their application to the structural characterization of both GaNAs and InGaNAs molecular-beam-epitaxy (MBE)-grown alloys, with particular emphasis on N lattice location; and second, their use in combination with other techniques in order to verify the validity of Vegard's rule in correlation to the nitrogen substitutional fraction of the epilayers. Our results indicate the validity of Vegard's rule and suggest that systematic errors can affect the measures, leading to incorrect conclusions.

The article is structured as follows: in Sec. II, details about the experimental setup of the adopted techniques will be described (MBE growth, NRA and RBS measurements, HRXRD); the following section is divided in three parts: Sec. III A describes the whole experimental procedure in order to obtain accurate results about N concentration; Sec. III B presents the results about the substitutional fractions, while Sec. III C describes the results about the relaxed lattice parameter obtained by HRXRD and elasticity theory. In Sec. IV, all the results are correlated together and discussed with a

[a]Electronic mail: berti@padova.infm.it

TABLE I. Summary of the samples and of their experimentally determined structural parameters.

Sample	Thickness (nm)[a]	x (%)[b]	y (%)[c]	$f_{[001]}$[d]	$f_{[111]}$[d]	a_x (Å)[e]
A	146	0	1.68±0.06	1.02	0.98	5.6323
B	147	0	1.93±0.06	1.03	···	5.6298
C	145	0	3.20±0.11	0.99	···	5.6194
D	130	0	4.45±0.13	1.00	···	5.6035
E	144	3.6	0	···	···	5.6671
F	154	4.1	1.57±0.06	0.99	···	5.6511
G	152	4.2	1.77±0.07	1.01	···	5.6493
H	145	4.3	1.81±0.07	1.03	1.01	5.6497
I	145	4.4	1.99±0.06	1.04	1.02	5.6484
L	140	4.3	2.00±0.07	0.96	···	5.6483
M	136	3.8	4.55±0.13	1.01	···	5.6157

[a]The thickness has been measured by the interference fringes in HRXRD rocking curves. The error is about 2 nm.
[b]The In concentration has been measured by 2.0 MeV ^{4}He RBS. The error is ±0.1 at. %.
[c]The N concentration has been measured by NRA.
[d]N substitutional fraction determined by channeling along the indicated direction. The error is ±0.02.
[e]Relaxed lattice parameter obtained by HRXRD and elasticity theory. The error is estimated to be $\pm(1-2)\times10^{-4}$ Å including the error on the elastic constants.

comparison to the existing literature data regarding Vegard's rule. Section V draws the conclusions.

II. EXPERIMENTAL PROCEDURE

A. MBE growth and sample preparation

The epilayers were grown on 3 in. (100) GaAs substrates by gas source MBE (GSMBE), after de-oxidation of the substrates at 590–600 °C. The samples (see Table I) consist of a 400–500-nm-thick GaAs buffer layer grown at 580 °C, and the appropriate 150-nm-thick GaN_yAs_{1-y} (samples A, B, C, and D), $Ga_{1-x}In_xAs$ (sample E), or $Ga_{1-x}In_xN_yAs_{1-y}$ (samples F, G, H, I, L, and M) epilayer grown at 400–425 °C. The V/III flux ratio is around 6. The GSMBE system is equipped with a rf plasma source to decompose N_2 into N active species, the latter being controlled by the plasma power and the N_2 flux. The plasma power is kept constant at 275 W when growing the nitrided layers. The N_2 flux is controlled by a capacitance gauge that measures the N_2 pressure (p_{N_2}) in the gas line. $p_{N_2}=180$ mTorr for samples A, B, F, G, H, I, and L and $p_{N_2}=280$ mTorr for the other samples.

In order to calibrate the NRA signal related to the N nuclear reaction, two samples were prepared. The first one consists of a Si_3N_4/Si layer produced by photo-chemical vapor deposition on a Si substrate.[13] The second one is a GaAs substrate, ion implanted with N at 200 keV and a dose of about 5×10^{17} at./cm^2. The use of these samples is described in Sec. III A.

B. NRA and RBS measurements

In order to measure the concentration and for depth profiling of low-mass atoms in a heavy matrix, resonant backscattering spectrometry[14] by using energetic He beams would be ideal. In fact, the enhancement of the cross section above the Rutherford value for the light element may allow extracting its backscattering (BS) signal from the background due to BS from the matrix, while the He energy loss is sufficient for depth profiling with depth resolutions on the order of a few tens of nanometers.

Unfortunately, the reported ratios of the N elastic cross section with respect to the Rutherford one are all below 100, and this value is not sufficient to detect 1 at. % N in GaAs. On the other hand, NRA is a well established technique[15] for materials analysis, and it has been determined long time ago that in the case of ^{14}N the most appropriate nuclear reactions are deuterium induced, that is, $^{14}N(d,p/\alpha)^{15}N/^{12}C$,[16] even though the low energy loss of the deuterium beam and of the high-energy reaction products leads to essentially no depth resolution. NRA and RBS analyses were performed with a deuterium beam in the energy range from 900 to 1250 keV at the CN accelerator of Laboratori Nazionali di Legnaro (Padova, Italy). The beam charge collection was performed by using the whole scattering chamber as a Faraday cup, reaching an accuracy better than 1%. The sample holder was a two-axis remote-controlled goniometer allowing channeling alignments with an accuracy of about 0.01°. Two translation movements are also available, allowing us to locate the beam spot (2 mm diameter) on the sample surface with an accuracy of a tenth of millimeter. Two silicon solid-state detectors were mounted in the chamber and connected with two independent acquisition electronic chains, allowing the simultaneous collection of NRA and RBS spectra. The RBS detector, mounted in the Cornell geometry at a scattering angle of 170° had a very small solid angle of about 0.8×10^{-4} strad, allowing us to keep the total counts per second below 4×10^3 s^{-1} with a beam current of about 200 nA. On the contrary, the NRA detector (300 mm^2) was mounted very close to the sample with a solid angle of about 0.3 strad, in order to maximize the nuclear reaction product count rate. A 19-μm-thick Mylar™ absorber was placed in front of this detector in order to avoid the RBS counting rate contribution. The NRA detector was positioned in the IBM geometry at a scattering angle of 150°. NRA and RBS spectra were collected both in random and in channeling geometry in order to determine the total concentration and the substitutional fraction of N. The random spectra were collected while rotating the sample around the selected axial direction, with an azimuth angle of 5°. This procedure allows the smoothing of every channeling effect and provides a result (random spectrum) that is equivalent to the one that would be obtained from amorphous samples.

RBS spectra were also collected with a 2 MeV $^4He^+$ beam in order to determine the In concentration and thickness of the InGaNAs epilayers, and to measure the N dose of the Si_3N_4/Si standard sample. The measured layer thicknesses and In concentrations are reported in Table I.

C. HRXRD measurements

HRXRD measurements were performed with a Philips X'PERT™ PRO MRD diffractometer equipped with a Bartels Ge (220) four-crystal monochromator and a parabolic mirror, using a channel-cut Ge (220) analyzer before the de-

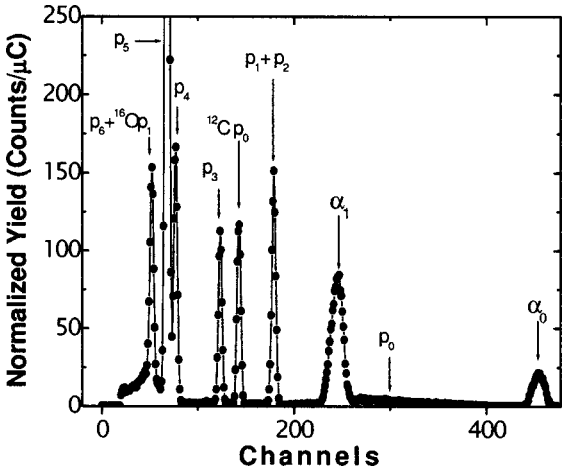

FIG. 1. Energy spectrum of the nuclear reaction products induced by a 1200 keV deuterium beam on the N-implanted GaAs sample. A 19-μm-thick Mylar absorber was put in front of the detector having a 300 μm depletion layer. The peaks marked with α are related to the $^{14}N(d,\alpha)^{12}C$ reaction, while peaks marked with p are related to the $^{14}N(d,p)^{15}N$ reaction (p_5 is out of scale). Also indicated is the $^{12}C(d,p)^{13}C$ peak, while the $^{16}O(d,p)^{17}O$ peak is not resolved from the $^{14}N(d,p_6)^{15}N$ peak.

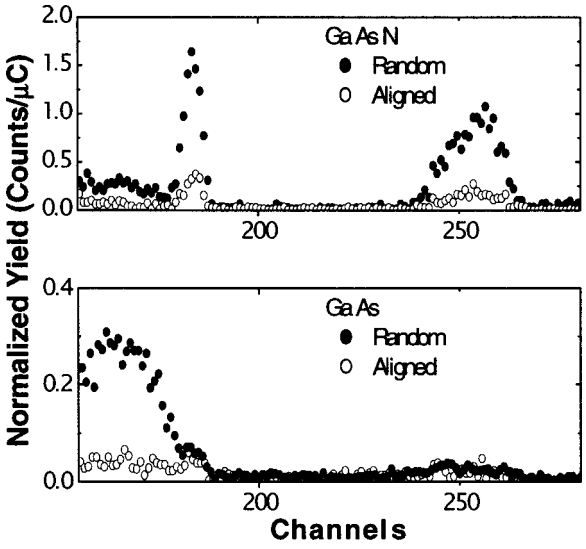

FIG. 2. NRA energy spectra in the range of the p_1+p_2 to α_1 peaks. In the upper and lower panel random and [001] aligned spectra for a GaNAs sample and a GaAs substrate, respectively, are shown. Note the different vertical scale in the two panels. A background contribution, clearly coming from GaAs (see the lower panel), ends close to the p_1+p_2 peak. A N contribution (p_1+p_2 and α_1 peaks) which is not influenced by channeling, is evident for the bare GaAs substrate and is attributed to a N submonolayer physisorbed at the surface.

tector (triple-axis configuration). The size of the x-ray beam at the sample was reduced by placing a mask after the monochromator, obtaining a probe of $3\times0.5\ mm^2$. Special care was adopted to laterally align the sample and to perform both NRA and XRD analyses on the same point of the sample in order to minimize errors due to sample nonhomogenity. First of all, reciprocal space maps (RSMs) were collected in order to test the possible presence of tilt and the pseudomorphicity of films. Rocking curves were also recorded, in order to determine the lattice parameter of the epilayers and, from the Pendellossung fringes, their thickness. The measured thickness of the layers is reported in Table I.

III. RESULTS AND DISCUSSION

A. Composition measurements

A typical NRA spectrum collected from the N-implanted GaAs standard sample with a 1200 keV deuterium beam is shown in Fig. 1. A series of nuclear reaction products are visible in the spectrum. At the highest energies (channels), the α_0 peak from the $^{14}N(d,\alpha_0)^{12}C$ reaction can be observed, while the much more intense α_1 reaction channel, relative to the first excited state of the ^{12}C nucleus, is visible around the channel 250. The p_0 symbol indicates the $^{14}N(d,p)^{15}N$ reaction product relative to the fundamental state of the ^{15}N nucleus. This signal is spread over the channel range between 200 and 400 because of the high energy of such proton group, which is not stopped in the detector depletion layer (300 μm). Only a fraction of the proton energy is deposited in the detector, and this fraction widely varies because of the energy straggling of the protons in the detector. This signal could be well separated from other peaks by a detector with a higher depletion layer, but it does not influence our measurements because its background contribution to the α_1 peak is proportional to the N amount.

The other proton peaks are narrower than the α peaks because of the lower energy straggling of protons in the Mylar absorber with respect to that of α particles. The p_1 and p_2 peaks form a doublet that appears in the spectrum as a single peak around the channel 180. At lower energies, the proton peaks from $^{14}N(d,p)^{15}N$, $^{12}C(d,p)^{13}C$ and $^{16}O(d,p)^{17}O$ are identifiable. The contribution from surface carbon is an isolated peak around channel 150, at energies higher than the p_3 peak from ^{14}N. Higher order proton peaks from N together with the p_1 from oxygen can be observed in the low energy part of the spectrum and are not (completely) resolved. Due to the low oxygen contamination and to the small cross section, the p_0 peak from $^{16}O(d,p)^{17}O$ does not contribute to the spectrum.

The choice of the reaction products to be used in the analysis can be restricted to the p_1+p_2 and the α_1 peaks because of the lower cross section relative to the α_0 peak and because of the possible interference of other impurity peaks with N peaks at energies below the C peak. This fact becomes critical when the N amount is very low (in the epilayers under investigation the N amount, that is, the nitrogen peak intensity, is about two orders of magnitude lower than in the implanted sample).

In Fig. 2, a magnification of the spectrum in the energy range relative to the p_1+p_2 and α_1 peaks is shown for a GaNAs epilayer (upper panel) and for a GaAs substrate without any intentional N contamination (bottom panel). In each panel, both random and [001] aligned spectra are shown. As can be noted the p_1+p_2 peak appears to rise at the end of a continuous signal visible in all the spectra. This signal is clearly related to the GaAs substrate because it is present in both the GaAs substrate and the epilayer with the same intensity (note the different scale between the two panels).

Moreover, the signal has a strong reduction under the channeling condition, and it has been verified that it is independent of the doping impurities of the GaAs substrates. The high-energy tail of such signal is partially superimposed to the p_1+p_2 peak and can affect its integral by as much as 10% for 2 at. % GaNAs. As this signal is clearly not related to N, this interference would introduce a systematic error in the N determination not acceptable for the purpose of this work. Thus, we based our work on the α_1 peak.

Another interesting piece of information coming from Fig. 2 concerns the small peaks visible in the lower panel (GaAs substrates) corresponding to both p_1+p_2 and α_1 peaks. These signals, which do not change under channeling or random conditions, can only be due to a N surface contamination of the GaAs substrate. This contamination perturbs the evaluation of the N amount in the epilayers, especially at very low N doses, and becomes even more critical when channeling spectra are used to evaluate the substitutional fraction.

In order to take into account and to minimize this effect, particular care was taken in order to clean the surface by organic contaminants. However, it was not possible to eliminate it. Some GaAs samples, which underwent the best cleaning procedures, were measured in different positions on the surface both in channeling and in random conditions. The total amount of contaminant N was found to be $(2\pm1)\times10^{14}$ at./cm^2, where the uncertainty indicates the point to point variability of the measurements and not only the statistical error. This quantity has been assumed to correspond to a fraction of N monolayer physisorbed at the surface, and in the following, it will be taken into account in the analysis of the spectra obtained from the epilayers.

It must be underlined that this contamination, being unaffected by channeling, if not corrected, would give rise to an apparent fraction of interstitial N. In Ref. 12, for total N concentrations varying from about 1 to 3.5 at. %, surprisingly, a nearly constant N interstitial concentration of 2.2×10^{19} at./cm^3 was found. For the thickness of those samples (100 nm) this concentration corresponds to a N amount of 2.2×10^{14} at./cm^2, exactly the value we found for the surface contamination. We thus believe that this reported interstitial N concentration is not related to N in the epilayers, but to the N surface contamination.

The previous results allow concluding that the most suitable nuclear reaction channel for quantitative analysis of very small amounts of N in a GaAs matrix is the α_1 channel. It is reported[15] that the cross section of this reaction at 150° is almost constant in the energy range between 1050 and 1400 keV. In our scattering geometry, the NRA detector spans a very large angular range, so that it was necessary to verify the energy dependence of the cross section integrated over our large solid angle.

In Fig. 3, the counts per unit charge from the α_1 peak of the N-implanted GaAs sample are reported as a function of the energy in the range between 900 and 1250 keV. The energy in the abscissa corresponds to the beam energy minus the average energy lost in the implanted region. This energy loss was calculated on the basis of Ziegler's stopping power table.[17] This table is obtained by extrapolating data through a master equation because no direct measurements of D energy loss in GaAs are available in our range of interest. In order to check the reliability of the tabulated values, both deuterium and helium RBS spectra relative to the N-implanted GaAs sample were successfully simulated by using the same N depth profile, thus indicating the consistency of the D stopping values with those of He. In fact, in the ion-implanted calibration sample, the N concentration deduced from the TRIM code[18] is about 40 at. %. This concentration is not sufficient to give a distinct N BS signal on the GaAs background, but it is sufficient to produce a measurable dip of the GaAs yield in the implanted region. The size of this dip is not very sensitive to changes in N concentration, so that this analysis does not supply a sufficiently reliable concentration profile. However, the energy position of the dip in the spectrum depends on the stopping power. On the other hand, He stopping in GaAs is reliable within a 4% relative error according to a cross check between layer thicknesses measured by 2 MeV $^4He^+$ RBS and from transmission electron microscopy cross sections.[19]

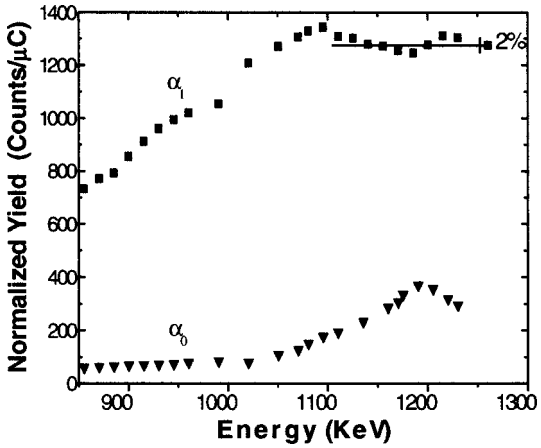

FIG. 3. Total yield integrated over the α_1 (squares) and the α_0 (triangles) peaks of the $^{14}N(d,\alpha)^{12}C$ reaction as a function of energy. The α_1 reaction channel shows an almost constant yield ($\pm2\%$) in the 1100–1250 keV range.

As can be noted from Fig. 3, the α_1 yield is constant within $\pm2\%$ in the energy range between 1100 and 1250 keV allowing us to measure with nearly constant sensitivity about 2 μm of GaAs. Within this thickness, the calibration sample and the epilayers can be measured introducing negligible errors due to the different energy losses. Moreover, this fact permits neglecting the difference in energy loss when collecting random or aligned spectra.

The last step to make the NRA technique quantitative is to convert the yield of the reaction into a N dose. The Si_3N_4/Si standard was first calibrated by 2 MeV $^4He^+$ RBS measurements supplying a N dose of $(2.97\pm0.08)\times10^{17}$ at./cm^2. The determination of the N dose has been performed by measuring the integral of the N signal, which can be best isolated from the Si background in channeling configuration. The N integral is then converted to an areal density by calibrating the RBS solid angle against the yield of a standard sample whose composition is known with a 2% accuracy.[20] The same procedure cannot be per-

formed directly on the N-implanted GaAs sample because of the higher background due to GaAs.

The N-implanted GaAs sample was calibrated as a secondary N standard by measuring the deuterium-induced nuclear products for both the Si_3N_4/Si and the N-implanted GaAs samples. This calibration is not possible at 1200 keV because of a very strong Si background of the silicon nitride sample below the α_1 peak (more than 100%). The α_0 peak has no Si background, but it is not suitable for calibration because of the variation in the cross section around this energy. The calibration of the secondary standard was thus performed with a beam energy around 900 keV. At this energy, the α_0 cross section is quite constant (see Fig. 3), and there is no background due to the presence of Si or GaAs substrates. On the other hand, the α_1 peak permits higher statistics, and at this energy, the background due to the Si substrate is strongly reduced (about 10% of the α_1 peak). In order to determine the ratio of the N content in the two samples, several spectra were collected with a beam energy between 880 and 920 keV in order to accurately characterize the cross section variation with energy. Spectra on a bare Si substrate were also collected for background subtraction purposes, and the average energy loss in the two standard samples were taken into account as described earlier in this section. The yield ratio of the Si_3N_4/Si sample to the N-implanted GaAs sample turns out to be 0.562 ± 0.007 and 0.564 ± 0.009 according to the α_1 and to the α_0 analyses, respectively. The N dose in the GaAs N-implanted sample, taking into account the overall calibration errors, is then $(5.24 \pm 0.20) \times 10^{17}$ at./cm^2.

This standard sample was used to obtain the N dose in the epilayers by simply evaluating the α_1 yield ratio at 1200 keV beam energy in random geometry. The N concentration can be finally evaluated by assuming a constant concentration profile and by measuring the layer thickness by the analysis of the interference fringes in the HRXRD rocking-curves and also by 2 MeV $^4He^+$ RBS in the case of In containing samples. The obtained N concentrations are reported in Table I.

B. Substitutional fraction measurements

The channeling technique allows measuring the substitutional fraction of an element in a given crystalline matrix. The basic idea is to compare the minimum yield χ_i of the given impurity (defined as the ratio between its channeling and the random yields) to the χ_M of the matrix, through the equation

$$f = \frac{1-\chi_i}{1-\chi_M}, \tag{1}$$

where f is the substitutional fraction.

As for N, χ_N can be easily evaluated from the NRA spectra by the ratio between the aligned and the random spectra (Fig. 2, upper panel) once these values are corrected for the yield coming from the surface contamination (see previous section). Due to the lack of depth resolution of the nuclear reaction, χ_N is the average minimum yield in the epilayer and must be compared to the corresponding quantity for the GaAs matrix. This is the reason the RBS spectra must be simultaneously collected.

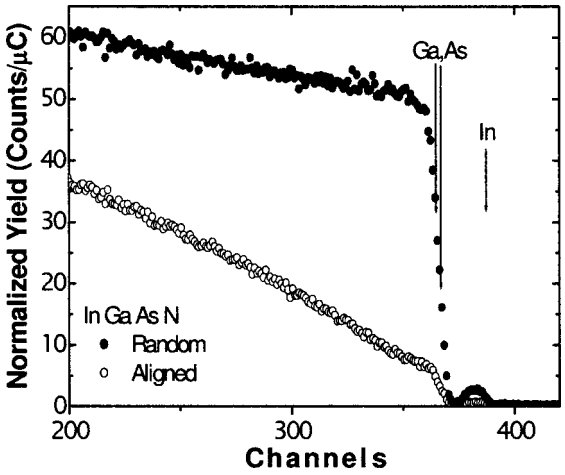

FIG. 4. Deuterium RBS spectra for an InGaNAs sample collected in random (closed circles) and [001] aligned (open circles) conditions. The arrows mark the energies for scattering from the indicated elements at the surface.

In Fig. 4, two RBS spectra, one aligned to the [001] direction and the other in random geometry are shown. The spectra are relative to an InGaNAs quaternary alloy, and both the In and GaAs signals are visible, allowing us to measure both χ_{In} and χ_{GaAs}. χ_{In} is obtained from the yield ratio of the In signal, while χ_{GaAs} is measured by the yield ratio in the energy window corresponding to that of In and taking into account the different kinematical scattering factors. This analysis showed, as expected, that In is fully substitutional. In the case of ternary alloys, χ_{GaAs} was measured by computing the energy window from the thickness of the layers (interference fringes in HRXRD rocking curves) and from the tabulated stopping powers.

The values of χ_{GaAs} found for GaNAs and InGaAsN are $\sim$9% and $\sim$10%, respectively. The value for InGaNAs higher than for GaNAs is consistent with a similar increase observed for InGaAs alloys with respect to GaAs and it is attributed to structural disorder around the In atoms. However, the measured GaAs minimum yields are higher than those typically observed. This is partially explained by the fact that our values are integrated over the layer thickness and are not, strictly speaking, surface minimum yields. Moreover, this integral includes the channeling surface peak, which is not resolved with the D beam. On the other hand, minimum yields for InGaNAs were also measured from 2 MeV He RBS and found to be about 6% and 4% by including or excluding, respectively, the contribution of the surface peak; that is, values consistent with those measured for high crystalline quality InGaAs alloys. We thus conclude that the high minimum yield values measured with the D beam are due to both the inclusion of the channeling surface peak and the angular divergence of our deuterium beam. The latter does not affect the measure of the substitutional fraction, as the reference GaAs RBS spectra were collected simultaneously with the N NRA spectra.

Finally, we must discuss the possibility of sample dam-

age during the measurements itself; that is, the possibility of lattice damage induced by the analyzing beam. It was demonstrated, for example, that $Si_{1-x}C_x$ alloys suffer of this effect and that it is particularly important for C yield.[21] In order to test this effect, repeated NRA channeling measurements were performed on the same spot. Effectively, in spite of the large beam diameter used, which allows us to reduce the ion fluence, the minimum yield increases with the integrated charge at a typical rate of 1.5%/100 μC. This rate of damage was taken into account in the data reduction. Similarly to the $Si_{1-x}C_x$ alloys case, this effect is much more pronounced for the N minimum yield than for that of the matrix and could introduce a large underestimate of the original substitutional fraction if not properly taken into account. Keeping the integrated charge below 100 μC, the influence of this effect in our samples is of the same order of the statistical error. Therefore, this amount of charge is a good compromise between accuracy and precision of the measurements. It is worth noting that the damage effect is much faster (more than 10 times) in random condition; it is therefore necessary to record aligned spectra on a virgin spot before recording the random one.

Applying the described data collection and data reduction procedure to our samples, we measured for all samples that all nitrogen atoms are substitutional along the [001] Ga or As rows within the error of measurement (see Table I). Strictly speaking, this procedure of evaluating the substitutional fraction does not take into account the possible presence of N point defects in which the interstitial N atoms are aligned along the [001] growth direction. In order to give a more complete characterization of the samples, channeling measurements were also repeated along the [111] axial direction for some selected samples, obtaining again full substitutionality for all the measured samples (see Table I).

In order to better understand these results, we considered a series of possible N point defects. The first one is N substitutional in a Ga site (N_{Ga}) instead of an As site (N_{As}). Of course, channeling measurements cannot distinguish between these two lattice locations as they are shadowed along the Ga or As rows. However, Orellana *et al.*[22] showed that the formation energy of N_{Ga} is much higher than that of N_{As}, so that the N_{Ga} location can be reasonably excluded.

Secondly, we considered tetrahedral and octahedral interstitial sites. The latter are displaced from ⟨001⟩ or ⟨111⟩ atomic rows by large and significantly different distances, so that yield differences in [001] or [111] channeling should be observed, which is not our case. As for the tetrahedral interstitial sites they are shadowed along GaAs rows for both ⟨100⟩ and ⟨111⟩ direction, so that our measurements cannot exclude their presence. However, Li *et al.*[9] reported that the formation of isolated interstitial N is unlikely because of its high formation energy in the lattice.

Thus, we further considered both ⟨100⟩ and ⟨110⟩ split interstitials on the basis of the structural model of Ref. 9 based on the covalent radii of the atoms. For both interstitial types, a significant fraction (ranging from 1/3 to 2/3) of the interstitials are displaced from ⟨001⟩ and ⟨111⟩ GaAs rows by distances of the order of the N covalent radius (i.e., by much larger distances than the thermal vibration amplitude and the Thomas–Fermi screening radius), so that they would not be shadowed in our measurements.

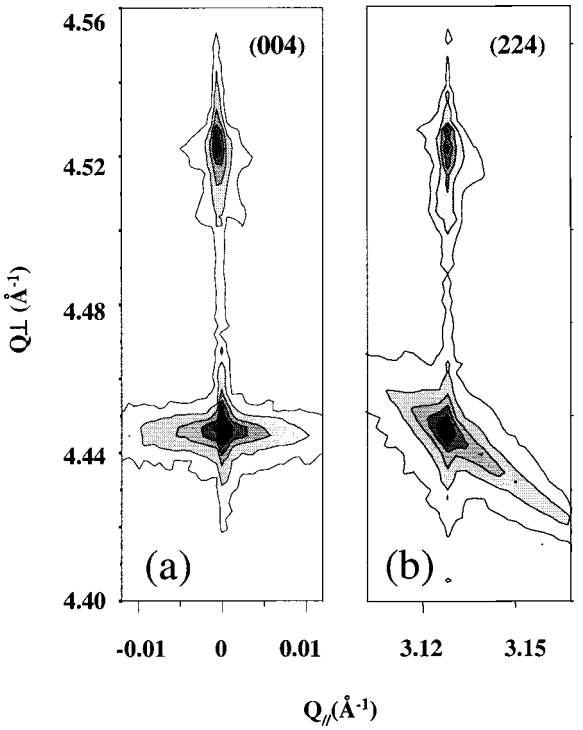

FIG. 5. RSMs around the (0 0 4) (a) and (2 2 4) (b) reflections of the most strained GaNAs sample. The isointensity contours are drawn in the range from 2 to 20 000 counts in a logarithmic scale. The absence of tilt and the pseudomorphicity of the sample is evident.

For ⟨001⟩ split interstitials, the strain of coherently grown layers could induce their orientation along the [001] growth direction, so that they would be shadowed in the [001] direction. However, they are displaced by 0.6 Å from ⟨111⟩ rows, so that yield differences along the two directions should be observed, contrary to our measurements.
From the previous discussions and within the sensitivity limit of the channeling technique, we can thus exclude the presence of N interstitials in our samples.

C. Lattice parameter measurements

The lattice parameter of the epilayers was determined by HRXRD measurements. Both rocking-curve measurements and RSM were performed. In Figs. 5(a) and 5(b), RSMs around the (004) and (224) reflections, respectively, are shown. These maps are relative to the most strained sample; that is, the GaNAs layer with the highest N content (4.5 at. %). The two pairs of peaks observed are relative to the substrate and to the tensile strained film. The pair of peaks in the (004) RSM is perfectly aligned along the perpendicular direction of the reciprocal space, indicating that there is no tilt between the epitaxial film and the substrate. The pair of peaks in the (224) RSM is also well aligned along the perpendicular reciprocal space direction, indicating that the sample is pseudomorphic. Thus, we can conclude that the value of the in-plane lattice parameter $a_{\parallel}$ of the films is equal to that of GaAs substrate.

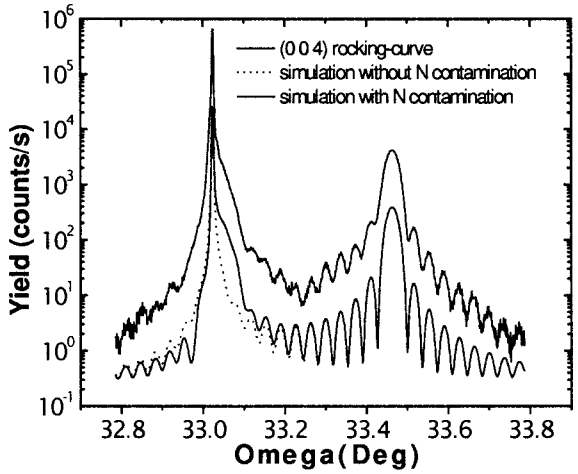

FIG. 6. (0 0 4) rocking curve of the GaNAs sample with 3% N. The presence of interference fringes show the good quality of the interface. The simulation marked with the dashed line is obtained by assuming a constant N concentration in the film, while the simulation marked with the continuous line takes into account a N contamination of the buffer layer.

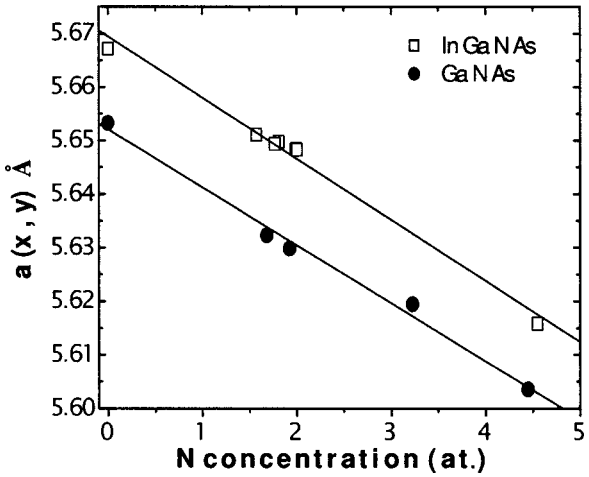

FIG. 7. Relaxed lattice parameter of epilayers as a function of nitrogen concentration. The closed symbols represent the ternary GaNAs alloy samples, while open symbols represent the quaternary alloys samples. The two continuous lines represent the linear fit to the two data sets.

In Fig. 6, the (004) rocking curve for a GaNAs sample with 3% N is shown. The presence of the interference fringes demonstrates the good crystalline quality of the material and of the interface. The simulation of the rocking curve by using the dynamical x-ray scattering theory based on the Takagi–Taupin equations allows us to obtain the perpendicular lattice parameter and the thickness of the layer. The simulation reported in Fig. 6 with a dashed line was obtained by assuming a constant concentration of nitrogen in the film. The good quality of the simulation is evident, except in the region around the substrate peak, where a tensile tail is visible. This part of the spectrum can be simulated as well (continuous line in Fig. 6) by assuming a tensile strain contribution coming from the buffer layer. It was already reported[8] that the buffer of samples grown in similar conditions results to be slightly contaminated by N, and this was confirmed by SIMS analysis. The simulation allows to quantitatively determine the amount of strain produced by this contamination. The strain profile is then converted to a N concentration profile: the typical dose of this contamination is 3×10^{14} at./cm^2. These data, available for all the samples, will be used to correct the epilayer N doses determined by NRA analysis that, as a matter of fact, integrates over the whole N amount without distinguishing between epilayer and buffer layer contribution.

The obtained information about the perpendicular and parallel lattice parameters ($a_\perp$ and $a_\parallel$) of the films can be used to obtain the relaxed lattice parameter $a(x,y)$ by applying elasticity theory:

$$a(x,y)=\frac{a_\perp+\alpha a_\parallel}{1+\alpha}, \tag{2}$$

where x and y are the In and N molar fractions, respectively, and $\alpha=2C_{12}/C_{11}$ is a function of the elastic constants C_{11} and C_{12} of the material. The elastic constants were determined by linear interpolation of the elastic constants of the limit compounds InAs, GaAs, and zinc-blende GaN.[23,24] The measured values of the relaxed lattice parameter $a(x,y)$ are reported in Table I.

IV. LATTICE PARAMETERS AND VEGARD'S LAW

As N in our samples was fully substitutional, we can safely determine the dependence of the lattice parameter versus composition of the ternary and quaternary alloys.

In Figure 7, the lattice parameters of the samples are reported as a function of the N composition. Two different series of data can be observed. The first one (closed symbol) is relative to the GaNAs ternary alloys. The second one concerns samples of quaternary alloys with an average indium content of about 4 at. %. As can be seen, the two sets of data draw two linear trends with different intercepts corresponding to the GaAs and to the InGaAs lattice parameters. The slopes turn out to be (-1.08 ± 0.06) Å and (-1.14 ± 0.05) Å for GaNAs and InGaNAs respectively; that is, they are the same within the errors of measurement.

The parallel trend indicates that the effect of N on the lattice parameter is independent of the indium content in this range of composition. The lattice parameter of both sets of data can therefore be described by the following linear relation:

$$a(x,y)=a_{\mathrm{GaAs}}+\Delta a_{\mathrm{In}}x+\Delta a_{\mathrm{N}}y, \tag{3}$$

where Δa_{In} is equal to $a_{\mathrm{InAs}}-a_{\mathrm{GaAs}}=0.405$ Å, while Δa_{N} is the parameter describing the deformation of the lattice parameter due to nitrogen in the alloy. In order to determine Δa_{N} from all the experimental data, Eq. (3) can be rewritten as

$$a(x,y)-(a_{\mathrm{GaAs}}+\Delta a_{\mathrm{In}}x)=\Delta a_{\mathrm{N}}y. \tag{4}$$

The term on the left of Eq. (4) can be evaluated for every experimental point. In fact, $a(x,y)$ is determined by HRXRD, x is measured by RBS, and a_{GaAs} and Δa_{In} are known from the literature. This term depends linearly on the nitrogen concentration y (measured by NRA) through the

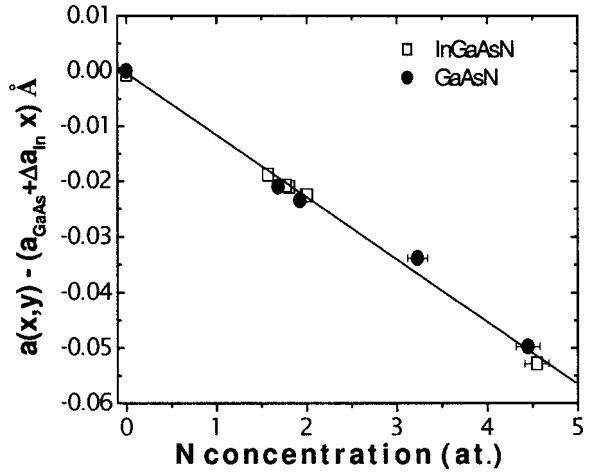

FIG. 8. Lattice contraction due to N for all the samples as a function of N composition. The continuous line is a fit to the data according to Eq. (4). Closed and open symbols refer to ternary and quaternary alloy samples, respectively.

coefficient Δa_N. In Fig. 8, $a(x,y)-(a_{GaAs}+\Delta a_{In}x)$ is plotted against y. The linear fit of all the data provides the estimate $\Delta a_N=(-1.12\pm0.02\pm0.04)$ Å, where the first and second errors correspond to the statistical uncertainty and to the systematic error introduced by the standard sample calibration procedure, respectively.

It is worth noting that, because the y values are small, the linear behavior could correspond to the initial slope of a curve, so that the experimentally determined Δa_N could include a bowing term, as found in other semiconductor alloys.[25–27] However, our result is in perfect agreement with the value of Δa_N predicted by Vegard's rule i.e., $\Delta a_N = a_{GaN}-a_{GaAs}=-1.13$ Å), demonstrating that the bowing term is null and that the lattice parameter of GaNAs and InGaNAs alloys is perfectly described by the Vegard's rule, at least in the investigated composition range and for fully substitutional N. This result is also in agreement with the computation of Neugebauer and Van de Walle.[10]

However, our results are different from those reported in Refs. 2, 9, and 11, where significant deviations from the Vegard's rule have been reported and explained on the basis of a possible interstitial N fraction. We stress here that single interstitials should lead to no strain;[28] N-N split interstitials should induce no strain[28] or should strongly reduce the tensile strain[9] as compared to N_{As}; and N-As split interstitials would give rise to compressive strain of the same order of magnitude of the tensile strain induced by N_{As}.[11] This means that, independently of N arrangement into the host lattice, a fraction of N interstitials should lead to less tensile strain (larger lattice parameter) with respect to substitutional N.

In this view, the results of Refs. 2 and 11 are consistent with the hypothesis of N interstitials. Unfortunately, the N lattice location in these papers was not investigated. On the other hand, the results of Ref. 9 are inconsistent with hypothesis of N interstitials because their deviation is opposite as that expected. This anomalous behavior could be explained by a matrix effect in their SIMS measurements of the total N concentrations.[29]

Finally, we consider that our measurements indicate that N is fully substitutional within the error of measurement; that is, we can affirm that at least 98% of the N atoms in the epilayers are in substitutional sites independent of nitrogen concentrations. If any, the remaining interstitial fraction would affect the slope of Fig. 8 with an error of +2%–4% (depending on the type of interstitials) which is, in any case, within our combined error bar. On the other hand, by assuming, as in Ref. 11, that the N interstitial concentration is proportional to the square of the N concentration and their proportionality parameter is adopted, in our samples we should have more than 2% interstitials above 2.6 at. % N concentration, and this fraction should reach nearly 6% for the highest concentration investigated (4.5 at. %). This fraction, if present, should have been observed.

In conclusion, our work demonstrates that Vegard's rule is followed in substitutional N nitride-arsenide alloys as theoretically predicted,[10] and that the maximum fraction of interstitial N in our samples is no more than 1%–2% of the N concentration.

V. CONCLUSIONS

In summary, we have performed a careful determination of concentration and lattice location of nitrogen in a series of GaN_yAs_{1-y} and $In_yGa_{1-y}N_xAs_{1-x}$ epilayers with different N and In concentrations ($0.015<x<0.045$) grown pseudomorphically on GaAs (001) substrates. The concentration of nitrogen of the samples was measured by NRA using the $^{14}N(d,\alpha_1)^{12}C$ reaction. In all the samples nitrogen was found fully substitutional. The correlation of the N concentration to the lattice parameter of the epilayers obtained from HRXRD measurements shows a good agreement with Vegard's rule for both ternary and quaternary alloys.

ACKNOWLEDGMENTS

The authors wish to thank E. Napolitani for SIMS measurements and A. Sambo for technical assistance.

[1] W. Li, M. Pessa, T. Ahlgren, and J. Decker, Appl. Phys. Lett. **79**, 1094 (2001).
[2] S. Spruytte, C. Coldren, J. Harris, W. Wampler, P. Krispin, K. Ploog, and M. Larson, J. Appl. Phys. **89**, 4401 (2001).
[3] M. Kondow, T. Kitatani, M. C. Larson, K. Nakahara, K. Uomi, and M. Inoue, J. Cryst. Growth **188**, 255 (1998).
[4] R. Bath, C. Caneau, L. Salamanca-Riba, W. Bi, and C. Tu, J. Cryst. Growth **195**, 427 (1998).
[5] S. Sato, Y. Osawa, and T. Saitoh, Jpn. J. Appl. Phys. **36**, 2671 (1997).
[6] M. Kondow, S. Nakatsuka, T. Kitatani, Y. Yazana, and M. Okai, Electron. Lett. **32**, 2244 (1996).
[7] W. G. Bi and C. W. Tu, Appl. Phys. Lett. **70**, 1608 (1997).
[8] L. Grenouillet, C. Bru-Chevalier, G. Guillot, P. Gilet, P. Ballet, P. Duvaut, G. Rolland, and A. Million, J. Appl. Phys. **91**, 5902 (2002).
[9] W. Li, M. Pessa, and J. Likonen, Appl. Phys. Lett. **78**, 2864 (2001).
[10] J. Neugebauer and C. Van de Walle, Phys. Rev. B **51**, 10568 (1995).
[11] W. J. Fan, S. F. Yoon, T. K. Ng, S. Z. Wang, W. K. Loke, R. Liu, and A. Wee, Appl. Phys. Lett. **80**, 4136 (2002).
[12] T. Ahlgren, E. Vaionen-Ahlgren, J. Likonen, W. Li, and M. Pessa, Appl. Phys. Lett. **80**, 2314 (2002).
[13] M. Berti, M. Meliga, G. Rovai, S. Stano, and S. Tamagno, Thin Solid Films **165**, 279 (1988).
[14] M. Berti, D. De Salvador, A. V. Drigo, F. Romanato, A. Sambo, S. Zerlauth, J. Stangl, F. Schaffler, and G. Bauer, Nucl. Instrum. Methods Phys. Res. B **143**, 357 (1998).

[15] *Ion Beam Handbook for Material Analysis*, edited by J. W. Mayer and E. Rimini (Academic Press Inc., New York, 1977).
[16] G. Amsel and D. Davies, Rev. Phys. Appl. **4**, 383 (1969).
[17] J. F. Ziegler, J. P. Biersack, and U. Littmark, *The Stopping and Range of Ions in Solids*, in Stopping and Ranges of Ions in Matter Vol. 1 (Pergamon, New York, 1984).
[18] TRIM code is available at www.srim.org
[19] M. Mazzer, A. V. Drigo, F. Romanato, G. Salviati, and L. Lazzarini, Phys. Rev. B **56**, 6895 (1997).
[20] C. Cohen, J. A. Davies, A. V. Drigo, and T. E. Jackman, Nucl. Instrum. Methods **218**, 147 (1983).
[21] M. Berti, D. De Salvador, A. V. Drigo, F. Petrovich, J. Stangl, F. Schaffler, S. Zerlauth, G. Bauer, and A. Armigliato, Micron **31**, 285 (2000).
[22] W. Orellana and A. C. Ferraz, Appl. Phys. Lett. **78**, 1231 (2001).
[23] O. Madelung, *Semiconductors Basic Data* (Springer, Berlin, 1996).
[24] V. Bougrov, M. E. Levinshtein, S. L. Rumyantsev, and A. Zubrilov, in *Properties of Advanced Semiconductor Materials GaN, AlN, InN, BN, SiC, SiGe*, edited by M. E. Levinshtein, S. L. Rumyantsev, and M. S. Shur (Wiley, New York, 2001), pp. 1–30.
[25] C. Bocchi, S. Franchi, F. Germini, A. Baraldi, R. Magnanini, D. De Salvador, M. Berti, and A. V. Drigo, J. Appl. Phys. **86**, 1298 (1999).
[26] M. Berti, D. De Salvador, A. V. Drigo, F. Romanato, J. Stangl, S. Zerlauth, F. Schaffler, and G. Bauer, Appl. Phys. Lett. **72**, 1602 (1998).
[27] D. De Salvador, M. Petrovich, M. Berti, F. Romanato, E. Napolitani, A. V. Drigo, J. Stangl, S. Zerlauth, M. Muhlberger, F. Schaffler, G. Bauer, and P. C. Kelires, Phys. Rev. B **61**, 13005 (2000).
[28] N. F. Chen, Y. Wg, H. He, and L. Lin, Phys. Rev. B **54**, 8516 (1996).
[29] E. Napolitani, D. De Salvador, G. Bisognin, M. Berti, and A. V. Drigo (unpublished).